



A Comparative Molecular Field Analysis and Molecular Modelling Studies on Pyridylimidazole Type of Angiotensin II Antagonists

Sung-eun Yoo,^{a,*} Soo-Kyung Kim,^a Sung-Hou Lee,^b Kyu Yang Yi^a and Dai-Woon Lee^c

^aBio-Organic Science Division 5, Korea Research Institute of Chemical Technology, P.O. Box 107, Yusung-gu, Daejeon, South Korea 305-606

^bScreening Division, Korea Research Institute of Chemical Technology, P.O. Box 107, Yusung-gu, Daejeon, South Korea 305-606

^cDepartment of Chemistry, Yonsei University, 134 ShinChon-Dong, SeoDaeMoon-Gu, Seoul, South Korea 120-749

Received 4 June 1999; accepted 10 August 1999

Abstract—A large number of compounds known as “AII (Angiotensin II) antagonists” have been developed for the treatment of various heart diseases such as hypertension, congestive heart failure, and chronic renal failure. Most of the currently known AII receptor antagonists share a similar chemical structure, consisting of nitrogen atoms, a lipophilic alkyl side chain and an acidic group. As a new series, we have designed and synthesized various pyridylimidazole derivatives. In this report we would like to discuss the structure–activity relationship of these series of compounds using the comparative molecular field analysis (CoMFA) methods. We could come up with a good CoMFA model (cross-validated and conventional r^2 values equal to 0.702 and 0.991, respectively) and the validity of the model was confirmed by synthesizing and measuring their biological activity of additional 6 compounds suggested by the model. This result provides additional information on the structural requirement for structurally diverse group of AII receptor antagonists. © 1999 Elsevier Science Ltd. All rights reserved.

Introduction

The role of the renin-angiotensin system (RAS) and its importance in the regulation of blood pressure in living systems are now well established.¹ The most active research in this field has been the development of non-peptidic antagonists for angiotensin II receptor² and recently numerous compounds possessing diverse chemical structures have been introduced as new receptor antagonists.^{3–5} Various pharmacophore models based on these diverse structures have been postulated with an unsolved question, whether these highly active molecules are binding at the same site of receptor.⁶

In our previous study, we tried to establish the three-dimensional arrangement of pharmacophoric elements for angiotensin II type I receptor antagonists with conformationally restricted derivatives of DuP753, a prototypic compound of angiotensin II antagonists.⁷ In the

case of DuP753, it was proposed that there are three pharmacophoric elements in the molecule; a nitrogen atom and an alkyl side chain in the imidazole ring, and an acidic tetrazole moiety and these elements are connected through the biphenyl group as a spacer. As a new class of antagonists, we have synthesized a number of pyridylimidazole derivatives and measured their AII binding activity. We have carried out 3D-QSAR studies using the comparative molecular field analysis (CoMFA) method introduced by Cramer,⁸ in order to understand the structural and conformational features of these compounds and also to obtain further insight into the relationship between the structure and biological activity. The CoMFA analysis that correlates the contribution of the steric and electrostatic fields with biological activity is expected to provide useful information on the environment around the binding site of the AII receptor.

Results and Discussion

In recent publications, there is strong evidence suggesting that in CoMFA the overall influence of the point

Key words: QSAR; CoMFA; antagonists; antihypertension.

* Corresponding author. Tel.: +82-042-860-7140; fax: +82-042-861-1291; e-mail: seyoo@pado.kRICT.re.kr

charges is not sensitive to the method of how these were calculated.⁹ However, in our case we found that especially in the series containing sulfur and nitrogen atoms, the predicted biological activities are quite dependent on how the charges were calculated. Therefore, we computed the partial atomic charges of all molecules using PM3 prior to the conformational analysis.

The correlation coefficient, which is the most widely used decisive factor for a valid analysis may vary considerably upon change of CoMFA parameters like the probe atoms, charge, grid space, cut-offs, grid locations and alignments. Since nearly all of the successful CoMFA analyses have been done with default parameters suggested by the CoMFA module, we also used default settings in our analysis.

A set of 32 compounds with specific biological activity (IC_{50}) values ranging over 3 orders of magnitude were used for a training set (Table 1). The test set of six new compounds was used for finding out the predicting

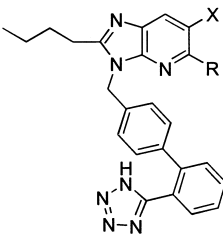
ability of the model (Fig. 1). We used the most stable conformer selected from the pool of conformers generated by the GRID module. Overlapping the common parts of the molecules using the method of database alignment, aligned the lowest energy conformations from each molecule. All molecules were superimposed well except varying R groups.

The results of the CoMFA studies for 32 training sets are summarized in Table 2. For pyridine *N*-oxide series (the model A), the CoMFA yielded a good correlation with cross-validated r^2 and conventional r^2 to be 0.699 and 0.931, respectively. In the case of the pyridine series (the model B), the CoMFA also yielded a correlation with cross-validated r^2 (0.603) and conventional r^2 (0.987). In model C, in which pyridine and pyridine *N*-oxide analogues were combined, even better correlation was obtained with cross-validated r^2 (0.702) and conventional r^2 (0.991). The relative contributions by the steric factor and the electronic factor were 63.1 and 36.9%, respectively. Since the steric interaction energy is changing much faster than the Coulomb interaction energy, a nonlinear behavior occurs which tends to statistically over-emphasize the steric field. Figure 2 shows a CoMFA map of the same structure embedded for all three models. The model B showed a quite different type of the CoMFA map from the models A and C. This result is quite consistent with the fact that most of outliers in the model C are from the compounds used in the model B. The CoMFA maps of the models A and C indicate that the R groups are better to bear more negative charge and *ortho* or *para* substitution of the pyridine ring is more favorable for a better activity. In contrast, the CoMFA map of the model B indicates that more positively charged groups are desired for a R group and substitution of less bulky group at pyridine ring is required in order to increase their activities.

Once the satisfactory CoMFA map was established, the QSAR Optimize Interface in the Advanced CoMFA module was used to build a series of analogues and to estimate expected activities chosen from 221 distinct substituents provided by Sybyl program. After reviewing 221 substituents for the R group, more than 25 substituents were suggested to have better activity than the groups used in the analysis (Table 3). With these 25 new suggested compounds, we then refined the CoMFA by performing further conformational study and the recalculation of atomic charge by the PM3 method. In the case of small and simple substituents, the predicted values from the refined model turned out to be quite similar to the initially predicted values. However, in the case of large bulky groups the two values were quite different depending on the conformations. Furthermore, in the case of substituents containing S, N and P atoms, the result is quite different depending on how the charge is calculated, by Gastieger-Huckel or PM3 method.

In order to validate the CoMFA model, we chose the nitrile group for R because of easy synthesis and small extrapolation that meant high predicting ability. We also synthesized additional regioisomers of pyridine *N*-oxide. With the experimentally obtained biological

Table 1. The pyridylimidazole derivatives for angiotensin II antagonists and their IC_{50} values



	R	X	IC_{50} (nM)
1	CH ₂ OH	1-oxo-pyridine-2-yl	0.82
2	CH ₂ OH	pyridine-2-yl	0.82
3	CH ₃	1-oxo-pyridine-2-yl	1.40
4	CH(OCH ₃) ₂	pyridine-2-yl	1.56
5	COOCH ₃	1-oxo-pyridine-2-yl	1.78
6	COOCH ₃	pyridine-2-yl	1.87
7	CH(OCH ₃) ₂	1-oxo-pyridine-4-yl	1.46
8	CH(OCH ₃) ₂	pyridine-4-yl	1.36
9	CH ₂ OH	1-oxo-pyridine-4-yl	0.86
10	CH ₂ OH	pyridine-4-yl	1.06
11	CH ₃	1-oxo-pyridine-4-yl	0.92
12	CH ₃	pyridine-4-yl	2.48
13	CH ₃	1-oxo-pyridine-3-yl	1.04
14	CH ₃	pyridine-3-yl	2.58
15	CH ₃	1-oxo-5-methylpyridine-2-yl	1.47
16	CH ₃	5-methylpyridine-2-yl	2.13
17	CH ₃	1-oxo-4-methylpyridine-2-yl	1.61
18	CH ₃	4-methylpyridine-2-yl	0.37
19	H	1-oxo-pyridine-2-yl	1.32
20	H	pyridine-2-yl	1.36
21	CH ₃	1-oxo-6-methylpyridine-2-yl	2.09
22	CH ₃	6-methylpyridine-2-yl	2.53
23	CH ₂ SO ₂ CH ₃	1-oxo-pyridine-2-yl	1.91
24	CH ₂ SO ₂ CH ₃	pyridine-2-yl	0.90
25	CHCH ₂	pyridine-2-yl	12.74
26	CH ₂ CH ₃	1-oxo-pyridine-2-yl	5.06
27	CH ₂ CH ₃	pyridine-2-yl	2.16
28	CH ₂ OCH ₃	1-oxo-pyridine-2-yl	1.42
29	COCH ₃	1-oxo-pyridine-2-yl	7.89
30	COCH ₃	pyridine-2-yl	1.78
31	CH(CH ₃) ₂	1-oxo-pyridine-2-yl	4.47
32	CH(CH ₃) ₂	pyridine-2-yl	12.69

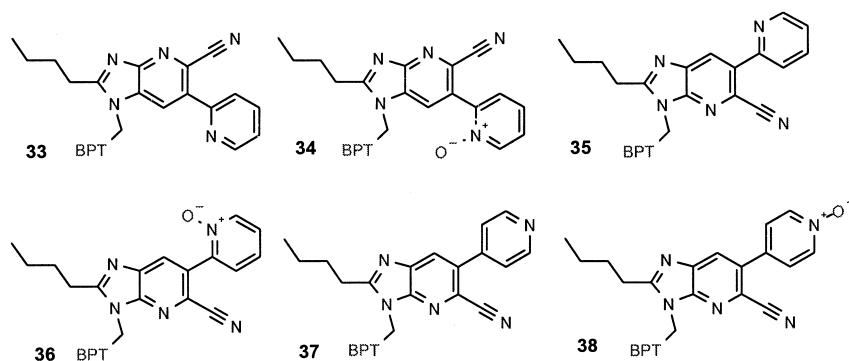


Figure 1. The structure of the compounds used in the test set. BPT is biphenyltetrazole.

Table 2. The summary of CoMFA-PLS results

	Model A	Model B	Model C	Model D
Total number of compounds used	16	16	32	38
The number of omitting compound	2	5	8	4
Cross-validated r^2	0.699	0.603	0.702	0.788
Number of component	3	3	5	4
Conventional r^2	0.931	0.987	0.991	0.964
Relative contributions				
Steric	54.5	41.9	63.1	50.8
Electrostatic	45.5	58.1	36.9	49.1

activity of 6 additional analogues, the predictive capability of models A, B and C was further examined. The predicted activities for 6 compounds excluded from the training set gave well predicted $r^2=0.8037$ (Fig. 3 and Table 4). Although predicted activity is little higher than the experimental activity, the tendency of predicted activity for all six compounds was good agreement with

experimental activity. As seen previously, the model of pyridine *N*-oxide series (the model A with predicted $r^2=0.8019$) shows better predicting ability than that of the pyridine series (the model B with predicted $r^2=0.2203$). The result reconfirmed that the cross-validated r^2 value is more important than the conventional r^2 value for measuring the predictability of the CoMFA model.

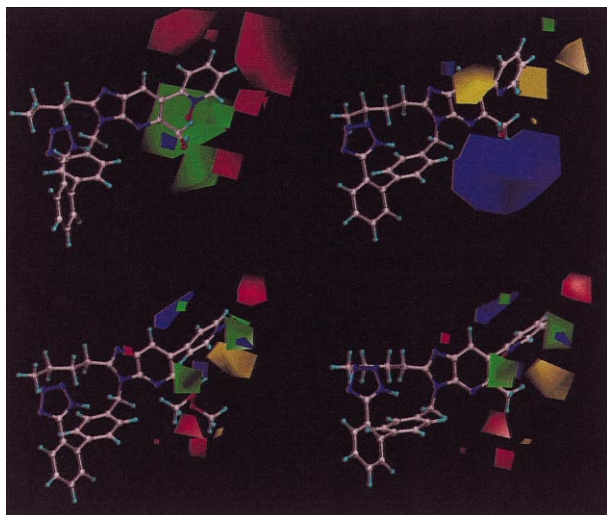


Figure 2. CoMFA map of pyridylimidazole derivatives for angiotensin II antagonist [Model A: Pyridine *N*-oxide series (upper left), Model B: Pyridine series (upper right), Model C: A and B mixed series (lower left), Model D: all series (lower right)]. The red and blue polyhedra indicate electrostatic contour plot. The regions where increased positive charge is favorable for activity are shown in blue, while regions where increased negative charge is favorable for activity are shown in red. The green and yellow polyhedra indicate steric contour plot. The regions where increased steric bulk is associated with enhanced activity are indicated in green, while regions where increased steric bulk is associated with diminished activity are indicated in yellow.

After removing outliers, the final CoMFA model including 6 additional compounds produced significant increased cross-validated and conventional r^2 values equal to 0.788 and 0.964, respectively. The final CoMFA map (the model D) turned out to be quite similar to that from the model C (Fig. 3 lower right). The relative contributions from steric and electrostatic are 58 and 49.1%, respectively. These results indicate that in our pyridylimidazole type of antagonists, the electrostatic interactions might play more important role in binding with the AII receptor and this result is also evident with the fact that charged or polarizable groups showed high predicted activity. It was also known that a variety of substituents at the imidazole C₄ and C₅ positions of DuP753 are not critical for binding, but, in general, a carboxylic group or other hydrogen bond-accepting substituents at C₅ such as a hydroxymethyl, carboxaldehyde, or carboxamido, group yield potent antagonistic activity.¹⁰ Our CoMFA map, when the H-bond field is used as a descriptors, indicates a region around the C₆ position of pyridylimidazole where a H-bond acceptor group is favorable. This result might be correlated nicely with the above SAR of DuP753. However, when the H-bond field was used as a sole descriptor ignoring the steric and electrostatic descriptors, it shows a poor statistical correlation (cross-validated r^2 : 0.454, conventional r^2 : 0.924). Since our

Table 3. The predicted IC_{50} 's of various substituents calculated by "optimizing QSAR" option of Sybyl. Because of high activity of *para*-substituted *N*-oxide series, only *para*-substituted *N*-oxides were used for the calculations. Only *R* groups that have a highly predicted activities are displayed

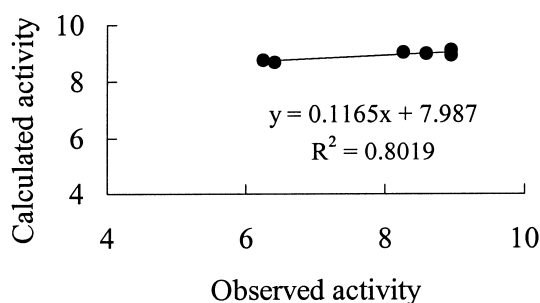
<i>R</i>	Predicted ($-\log IC_{50}$)	Extrapolation	Energy (kcal/mol)
PO_3H_2	9.41	0.18	45.89
O^-	9.39	0.47	27.45
CH_2COMe	9.35	0.02	18.55
PO_2H	9.35	0.29	9.59
$SCONH_2$	9.32	0.05	21.92
CHO	9.23	0.08	24.17
NO_2	9.22	0.15	14.05
NO	9.22	0.09	22.71
CH_2CCH	9.22	0.39	53.21
CF_2H	9.19	0.10	23.37
Br	9.18	0.05	25.00
Cl	9.18	0.06	25.44
CH_2F	9.18	0.08	25.20
$CHMeOH$	9.18	0.31	56.16
$SCONHMe$	9.17	0.12	26.57
SCN	9.16	0.05	23.13
I	9.14	0.07	24.74
CN	9.13	0.08	27.06
$SOCF_2H$	9.13	0.31	24.88
CF_3	9.12	0.09	21.51
F	9.11	0.08	27.99
<i>c</i> -Propyl	9.11	0.26	52.79
Methyl	9.10	0.06	25.73
CH_2CN	9.08	0.10	24.87
$POPh_2$	9.08	0.12	33.46
H	9.07	0.07	26.76
OH	9.06	0.05	26.18

pyridylimidazole analogues possess additional groups at the pyridine ring which are not available in most of previously known antagonists used for computational or CoMFA studies, our study will provide a useful information on possible additional binding site around that region. The docking model of DuP753 with AII receptor and parallel mutagenesis studies indicated that the C_5 position of imidazole locates around Ser107 in the helix3 of the AII receptor which seems to determine the subtype selectivity.^{11,12} Since the most of known antagonists used for the conformational and QSAR study lack proper groups, it has been difficult to study about the binding sites around that region. Therefore, CoMFA study of our pyridylimidazole analogues with various substituents at C_5 and C_6 will provide useful information around that region.

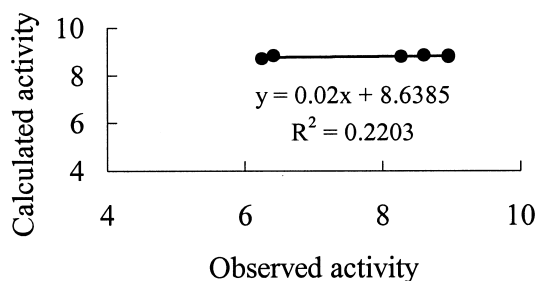
Conclusions

We have carried out the CoMFA analysis on the pyridylimidazole type of new angiotensin II antagonists. The CoMFA analysis showed good structure–activity relationships in a set of 36 pyridylimidazole analogues and also predicted accurately the biological activity of six new molecules. Although the CoMFA analysis works reasonably well in highly related congeners, we found that in a limited scope the CoMFA method is capable of predicting biological activity of unknown molecules that do not belong to the chemical class of compounds used for defining the training set. These

A. Model A



B. Model B



C. Model C

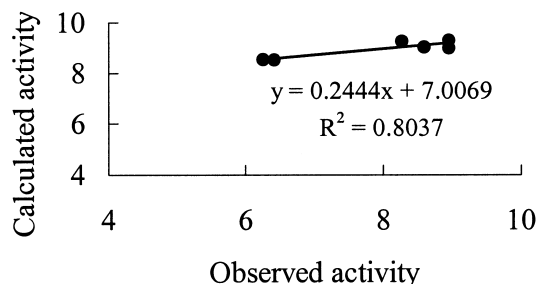


Figure 3. The predicting ability of three models (X: the experimental $-\log IC_{50}$ versus Y: the predicted $-\log IC_{50}$).

results will provide useful information in understanding the structural and electrostatic features of the angiotensin II receptor antagonists and in designing new antagonists.

Methods

Biological data

Binding assays were quadruplicated and performed in 96-well plates by incubating aliquots of the human recombinant AII receptor subtype I (BioSignal Inc.,

Table 4. The predicted and experimentally determined $-\log(\text{IC}_{50})$'s of six new compounds in the test set

No.	Experimental $-\log\text{IC}_{50}$	Predicted $-\log\text{IC}_{50}$ in Model A	Predicted $-\log\text{IC}_{50}$ in Model B	Predicted $-\log\text{IC}_{50}$ in Model C	Predicted $-\log\text{IC}_{50}$ in Model D
33	6.25	8.75	8.70	8.54	5.62
34	6.42	8.68	8.83	8.52	6.16
35	8.60	8.98	8.85	9.02	8.81
36	8.96	8.92	8.82	9.00	9.17
37	8.28	9.02	8.80	9.26	8.67
38	8.96	9.10	8.78	9.30	9.26

Canada) with 0.21 nM of [^{125}I] [Sar¹, Ile⁸]-AII. Test compounds were dissolved at 2.5 mM in dimethylsulfoxide and serially diluted to nine concentrations for the activity screening in total assay volume of 250 μL . The assay buffer contained 50 mM Tris, 5 mM MgCl_2 , 1 mM EDTA, 0.1% bovine serum albumin pH 7.4). Specific [^{125}I][Sar¹, Ile⁸]-AII binding was determined experimentally from the difference between counts in the absence and presence of 10 μM unlabelled.

After incubation at 37°C for 60 min, the incubation mixtures were filtered through glass-filter GF/C filters (Wallac, Finland) which were presoaked in 0.3% polyethylenimine and rapidly washed nine times with 200 μL of ice cold 50 mM Tris buffer (pH7.4) using the Inotech harvester (Inotech, Switzerland). The filters were covered with MeltiLex (melted on scintillator, Wallac, Finland), sealed in sample bag followed by drying in the oven, and counted by MicroBeta (Wallac, Finland).

The ability of antagonists to inhibit specific [^{125}I][Sar¹, Ile⁸]-AII binding was estimated by IC_{50} values, which are the molar concentrations of unlabeled drugs necessary to displace 50% of specific binding. The value for K_i was calculated from the equation (relationship between the inhibition constant (K_i) and the concentration of inhibitor which causes 50% inhibition (IC_{50}) of an enzymatic reaction) $K_i = \text{IC}_{50}/(1 + L/K_d)$, where L equals the concentration of [^{125}I][Sar¹, Ile⁸]-AII.¹³ The data from binding experiments were analyzed by the nonlinear regression, using the PRISM computer program (GraphPad Software Inc., San Diego, CA).

Molecular modelling

All molecular modelling techniques and CoMFA studies described herein were performed on Silicon Graphics workstations using the SYBYL (v. 6.4 from Tripos, Inc., St. Louis, MO).

A set of 32 compounds with specific biological activity (IC_{50}) values ranging over 3 orders of magnitude were used (Table 1). Atomic charges were calculated by the PM3 method.¹⁴ The database of molecules, the training set, was suitably aligned in 3 dimensional space according to the methodology of database alignment. The CoMFA analysis was performed using the QSAR module of Sybyl with the molecules embedded in a regularly spaced (2 Å grid box of 18×20×22 Å) (these values were determined by an automatic procedure performed by the Sybyl-CoMFA routine). Steric and electrostatic

interaction energies were calculated using sp^3 carbon probes with a +1 charge. After constructing the field, steric and electrostatic fields were calculated for each molecule by interaction with a probe atom at every grid points surrounding the aligned database in 3-D space. To correlate these field energy terms with their AII antagonistic activity, partial least squares (PLS)^{15,16} was used with cross-validation, giving a measure of the predictive power of the model. The final PLS analysis was performed using no cross-validation with an optimum number of components reported from the cross-validation result. The steric and electrostatic fields were scaled according to CoMFA standard deviation in order to give them the same potential weights on the resulting QSAR. The 3-D QSAR calibration model so derived was then used to predict the inhibitory activity of new compounds in the test sets (Fig. 1).

Replacing the R group with 221 substituents suggested by the CoMFA module optimized the final CoMFA.

Acknowledgements

We thank Tripos Associates for providing us the SYBYL program.

References

- Vallotton, M. B. *Trends Pharmacol. Sci.* **1987**, 8, 69.
- Carni, D. J.; Duncia, J. V.; Aldrich, P. E.; Chin, A. T.; Johnson, A. C.; Pierce, M. W.; Price, W. A.; Santella, J. B. III; Wells, G. J.; Wexler, R. R.; Wong, P. C.; Yoo, S.-E.; Timmermans, P. B. M. W. M. *J. Med. Chem.* **1991**, 34, 2525.
- Duncia, J. V.; Chiu, A. T.; Carini, D. J.; Gregory, G. B.; Johnson, A. L.; Price, W. A.; Wells, G. J.; Wong, P. C.; Calabrese, J. C.; Timmermans, P. B. M. W. M. *J. Med. Chem.* **1990**, 33, 1312.
- Kubo, K.; Kohara, Y.; Imamiva, E.; Sigiura, Y.; Inada, Y.; Furukawa, Y.; Nishikawa, K.; Naka, T. *J. Med. Chem.* **1993**, 36, 2182.
- Weinstock, J.; Keenan, R. M.; Samanen, J.; Hempel, J.; Finkelstein, J. A.; Franz, R. R.; Gaitanopoulos, D. E.; Girard, G. R.; Gleason, J. G.; Hill, D. T.; Morgan, T. M.; Peishoff, C. E.; Ayar, N.; Brooks, D. P.; Frederickson, T. A.; Offstein, E. H.; Ruffolo, R. R., Jr.; Stack, E. J.; Sulpizio, A. C.; Weidley, E. F.; Edwards, R. M. *J. Med. Chem.* **1991**, 34, 1514.
- Keenan, R. M.; Weinstock, J.; Finkelstein, J. A.; Franz, R. G.; Gaitanopoulos, D. E.; Girard, G. R.; Hill, D. T.; Morgan, T. M.; Samanen, J. M.; Peisoff, C. E.; Tucker, L. M.; Ayar, N.; Griffin, E.; Ohlstein, E. H.; Stack, E. J.; Weidley, E. F.; Edwards, R. M. *J. Med. Chem.* **1993**, 36, 1880.
- Yoo, S.-e.; Shin, Y. A.; Lee, S. H.; Kim, N. J. *Bioorg. Med. Chem.* **1995**, 3, 289.

8. Cramer, R. D. III; Patterson, D. E.; Bunce, J. D. *J. Am. Chem. Soc.* **1998**, *110*, 5959.
9. Folkers, G.; Mertz, A.; Rognan, D. In *3D QSAR in Drug Design: Theory, Methods and Applications*; Kubinyi, H., Ed.; ESCOM: Leiden, 1993; pp 584–618.
10. Wexler, R. R.; Greenlee, W. J.; Irvin, J. D.; Goldberg, M. R.; Prendergast, K.; Smith, R. D.; Timmermans, P. B. M. W.M. *J. Med. Chem.* **1996**, *39*, 625.
11. Prendergast, K.; Adams, K.; Greenlee, W. J.; Nachbar, R. B.; Patchett, A. A.; Underwood, J. J. *Comput. -Aided. Mol. Des.* **1994**, *8*, 491.
12. Ji, H.; Leung, M.; Zhang, Y.; Catt, K. J.; Sandberg, K. *J. Biol. Chem.* **1994**, *269*, 16533–16536.
13. Cheng, Y.; Prusoff, W. H. *Biochem. Pharmacol.* **1973**, *22*, 3099.
14. Leach, A. R. In *Reviews in Computational Chemistry*; Lipkowitz, K. B., Boyd, D. B., Eds.; VCH Publishers: New York, 1991; Vol. 2, pp 313–365.
15. Glen, W. G.; Dunn, W. J. III; Scott, D. R. *Tetrahedron Computer Methodology* **1989**, *2*, 349.
16. Stahle, L.; Wold, S. *Progr. Med. Chem.* **1988**, *25*, 292.